



Article

Geological Structures Controlling Au/Ba Mineralization from Aeromagnetic Data: Harrat ad Danun Area, Saudi Arabia

Kamal Abdelrahman ¹, Reda Abdu Yousef El-Qassas ², Mohammed S. Fnais ¹, Peter András ³ and Ahmed M. Eldosouky ^{4,*}

¹ Department of Geology & Geophysics, College of Science, King Saud University, P.O. Box 2455, Riyadh 11451, Saudi Arabia; khassanein@ksu.edu.sa (K.A.); mfnais@ksu.edu.sa (M.S.F.)

² Exploration Division, Nuclear Materials Authority (NMA), Cairo P.O. Box 530, Egypt; redaelqassas@yahoo.com or redaelqassas@nma.org.eg

³ Faculty of Natural Sciences, Matej Bel University in Banská Bystrica, Tajovského 40, 974 01 Banská Bystrica, Slovakia; peter.andras@umb.sk

⁴ Department of Geology, Suez University, Suez 43518, Egypt

* Correspondence: dr_a.eldosouky@yahoo.com or ahmed.eldosouky@sci.suezuni.edu.eg

Abstract: Positive and negative magnetic anomalies occupied the total aeromagnetic (TM) map of the Harrat ad Danun area, Saudi Arabia. Reduction to the pole (RTP) maps display the range of magnetic values (−312.4 to 209.4 nT) that vary in shape, size, and magnitude. These anomalies generally follow the NNW–SSE (Red Sea axis trend), NE–SW, and NNE–SSW trends. The NNW–SSE linear negative and positive magnetic anomalies could be brought on by buried faults, shear zones, or subsurface dikes. In the central part, the position of *Au* and *Ba* mineralization was connected to this trend. It is concluded that the principal structures are represented by the NNW–SSE, NE–SW, and NNE–SSW tendencies. Based on gridded RTP magnetic data, the 2-D power spectrum was computed and revealed the frequency of the near-surface and deep magnetic components. It is believed that the depths of the shallow and deep magnetic sources are typically 80 m and 570 m, respectively. Additional negative and positive magnetic anomalies with varied amplitudes and frequencies, trending in the NNW–SSE, ENE–WSW, and NE–SW directions, are seen when the high-pass and low-pass maps are closely examined. Many faults in various directions cut into these anomalies. The occurrence of negative linear magnetic anomalies (−36.6 nT to −137.3 nT) at this depth (80 m) is also confirmed by this map. The TDR filter and the Euler deconvolution method were used to identify the horizontal variations in magnetic susceptibility as well as the source position and depth of magnetic sources. The linear clustering rings are thought to be caused by contacts or faults with depths between 1 m to 474 m that are oriented WNW–ESE, NNE–SSW, and NNW–SSE. These faults or contacts are thought to be particularly prominent in the western, eastern, southern, northern, and central zones. The majority of felsic and mafic dikes are found to be connected to subsurface structures, showing that three structural trends—WNW–ESE, NNE–SSW, and NNW–SSE—affect the studied area. This demonstrates that important features and shear zones control the majority of Saudi Arabia’s gold deposits. A negative magnetic anomaly that is centered in the area, trending NNW–SSE and crossing the NNE–SSW fault, is connected to the plotted gold and barite mineralization in the study area. This may imply that these two tendencies are responsible for mineralization. This result raises the possibility of mineralization in the NNW negative magnetic feature located in the western part of the area. The occurrence of gold and barite was significantly impacted by the NNW–SSE and NNE–SSW structural lineaments.

Keywords: gold mineralization; aeromagnetic map; shear zones; Harrat ad Danun; Saudi Arabia



Citation: Abdelrahman, K.; El-Qassas, R.A.Y.; Fnais, M.S.; András, P.; Eldosouky, A.M. Geological Structures Controlling Au/Ba Mineralization from Aeromagnetic Data: Harrat ad Danun Area, Saudi Arabia. *Minerals* **2023**, *13*, 866. <https://doi.org/10.3390/min13070866>

Academic Editors: Javier Fernández Lozano and Erik Melchiorre

Received: 16 May 2023

Revised: 17 June 2023

Accepted: 23 June 2023

Published: 26 June 2023



Copyright: © 2023 by the authors. Licensee MDPI, Basel, Switzerland. This article is an open access article distributed under the terms and conditions of the Creative Commons Attribution (CC BY) license (<https://creativecommons.org/licenses/by/4.0/>).

1. Introduction

Saudi Arabia has not historically been known for its mining industry. Nonetheless, significant mining production has been observed at least three different times over

the past three thousand years [1]. The Abbasid Caliphate (750–1258 A.D.), the reign of King Solomon (961–922 B.C.), and the era of the Saudi Arabian Mining Syndicate (1939–1954) were the last three periods when gold was mined at Mahd ad Dahab, a mine that had produced gold intermittently since King Solomon's time and has been reopened since 1984 [2]. The former mining history of this nation is not reported in any other notable ways. Since 1947, Saudi Arabia has expressed interest in the use of its natural resources, but it was not until the 1950s and 1960s that infrastructure geology and exploration began in earnest. The massive entry of mineral raw materials into the post-World War II reconstruction of Europe at this time led to a boom in the global mining sector [3]. The Saudi Arabian government formed a separate ministry for petroleum and mineral resources in 1967 and provided it with a sizable budget, laying the groundwork for a well-organized program of mineral exploration. Since then, Saudi Arabia has pursued an aggressive exploration agenda with the help and assistance of some foreign agencies, resulting in the discovery of a diverse range of minerals, including precious and base metals, energy minerals (other than petroleum), industrial minerals, construction minerals, and ornamental stones. While some of these discoveries have already been turned into working mines, others are still being researched and investigated [4,5].

Saudi Arabia is acutely conscious of the need to diversify its economy and attain self-sufficiency in its many industrial sectors despite having 25% of the world's known oil reserves and deriving a fairly consistent income from them. Everything in their country's thinking and planning is based on this fundamental idea. Furthermore, it is believed that mineral resources and their exploitation are crucial to a nation's efforts to develop [2]. The development of mineral resources has also taken on a unique significance in Saudi Arabia given this context. Mineral development, on the other hand, will unleash a variety of benefits and multiplying effects into the process of national economic and social development. This will open up new doors for investment and the growth of other industries with the specific goal of extending their economic and industrial base. Saudi Arabia thus keeps up concerted efforts to look for, assess, and exploit its mineral resources.

There are two main geological settings in Saudi Arabia, each having a clear age and lithological difference. The Precambrian metamorphosed rocks from the Arabian Shield, the main source of mineral occurrences and discoveries, make up the western region of Saudi Arabia. The country's western region has exposed Shield rocks, which make up nearly one fourth of Saudi Arabia [6]. The alternative setting consists of more recent sediments from the Paleozoic, Mesozoic, and Tertiary eras that have not been altered or significantly disturbed. These cover rocks are dispersed across the north, east, and south of the Shield region and sit atop the stable Precambrian basement. Moreover, from the Tertiary to the present, there have been sporadic volcanic eruptions with some alkaline basaltic outflows, primarily in the Shield region. However, in Saudi Arabia, the most impressive Quaternary deposits are sands and gravels that cover rocks to create massive sand deposits [7–9].

The Shield area, which comprises stratiform deposits, veins, contact metamorphic deposits along the borders of igneous rocks, and magmatic and late magmatic deposits in igneous rocks, is the region with the best potential for finding metallic minerals. In contrast, non-metallic resources are dispersed across the entire nation, including the Shield, and are not limited to any particular region. Also abundant are several evaporites. The coastal region between the Red Sea and the Shield yields several minerals [6,10]. Investigation of the Red Sea's mineral deposits on the seabed has also produced promising results. In conclusion, Saudi Arabia offers a potential host environment that is rich in a range of metallic and non-metallic minerals, where numerous gold (Au) occurrences and other deposits have been found in the AS (more than 800); some of them, such as Mahd ad Dahab, Al-Sukhaibarat, and Bulghah, are currently in production [10,11]. In addition, the base metals (copper, zinc, and lead) are demarcated in select AS areas, such as Al-Nuqrah, Al-Amar, and Jabal Sayid [10].

The authors of [12] concluded that mining is crucial to the process of development because it transforms mineral resources into a form of capital that boosts a country's

output. Additionally, according to the conventional perspective, mining, like other economic activities, plays a vital role in the development process and may turn a mineral resource into sustained improvements in people's lives [13]. Together with the size of mineral resources over time, environmental costs, such as large amounts of solid waste, diminishing ore grades, energy, chemical, and water inputs, as well as pollution outputs, particularly greenhouse gases, are crucial components in determining how sustainable mining can proceed [8]. In order to properly control and encourage the sector's sustainable development, the Saudi government must increase the sectoral institutions' capabilities. A new mining code will also simplify the licensing processes and increase predictability and transparency by removing the administrative and legal barriers that prevent private sector participation in the minerals sector [14]. Recently, some research was conducted to assess Saudi Arabia's mineralization activities and structures [15–22]. Several areas in Saudi Arabia are promising because they hold great reserves of mineralization and have yet to be investigated in detail.

The magnetic survey was widely used in different applications such as mineral exploration, geological mapping, engineering, detect magnetic sources and their boundaries. Additionally, it was utilized to detect geologic structures (faults, contacts, folds, and shear zones) that might be relevant to the search for minerals [23–36].

2. Geological Setting

The study area is situated in Saudi Arabia's Western province, 158 km northeast of Jeddah. It covers the area between 21°50' and 21°56' north and 39°48' to 39°56' east (Figure 1a,b). The study area is situated in the Arabian Shield's western region. A simple geological map of the area under study (Figure 1c), which is a portion of the Makkah Quadrangle map created in [37], is shown in Figure 1c. A combination of metamorphic and plutonic rocks makes up the Western Arabian Shield, which includes the investigation area. The tertiary-layered rocks of the Rahat group make up the Harrat Rahat area, which serves as the region's southern boundary. Shaw Hit, Amah Basalt, and some alluvial debris make up this collection. Sedimentary rocks from the Tertiary period make up the lowest portion of the study area, which is covered in flows of basaltic lava. Precambrian–Cambrian complexes, Tertiary–Quaternary–Recent alluvial deposits, and Cretaceous–Tertiary sedimentary successions make up the area. Gabbro rocks in the east eventually ascend into Precambrian intrusions of biotite granodiorite and monzogranite from the north to the southeast [38]. The study area contains the following types of rocks:

1. Precambrian rocks: the Faiyadah Formation, which includes felsic volcanoclastic rocks, andesitic rhyolitic and basaltic lavas, as well as andesitic volcanoclastic rocks, is attributed to this group.
2. Precambrian intrusive rocks: belong to the Hishash Complex (igd), which is composed of granodiorite, and the Shiwan Complex (Kwtn), which is composed of hornblende tonalite.
3. Tertiary rocks: these rocks primarily come from the Haddat ash Sham (Tsh) and Hammah Basalt formations (Tmhb). Whereas the latter is made up of alkalic olivine basalt, the former is composed of pebbly sandstone and siltstone and is exposed in the study area's north and south.
4. Quaternary deposits: these make up a significant component of the study area and are mostly the result of weathering of the existing rocks. The alluvium's thickness varies from place to place, rarely exceeding 4 m in the study area's higher terrain while rising in the lower terrain and increasing to 29 m [37]. The Wadi Hishash soils are highly rich in quartz sand. In this region, the elevation decreases from 425 m to roughly 200 m. Pebbly sandstone and siltstone, which are composed of sand and gravel, surround the alluvial deposits.

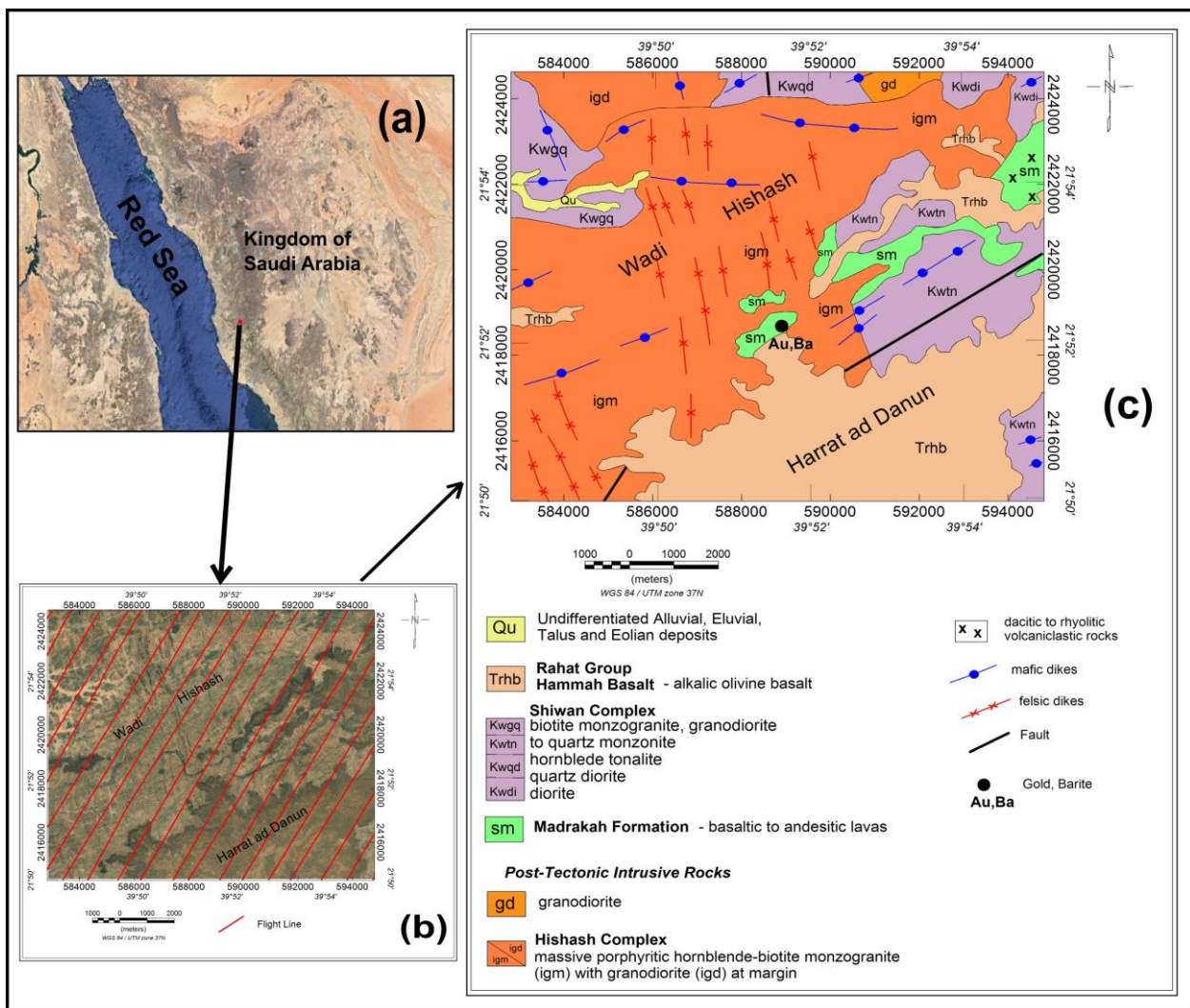


Figure 1. (a) Location map of Harrat ad Danun area, (b) Google Earth image, and (c) Geologic map of Harrat ad Danun area (after Moore and Al-Rehaili, 1989), Kingdom of Saudi Arabia.

3. Materials and Methods

The study area was flown by a consortium of Aero Service Corporation, Hunting Geology and Geophysics Limited, and Lockwood Survey Corporation Limited under the supervision of the Bureau de Recherches Géologiques et Minières for the Ministry of Petroleum and Mineral Resources of the Kingdom of Saudi Arabia between 1965 and 1966. This survey was carried out by the Fluxgate Gulf Mark III magnetometer with analog recording. The aeromagnetic survey flight lines were flown along parallel traverse lines oriented in a NE–SW direction, with an azimuth of 30° from true north and 800 m spacing. The tie lines were flown in an NW–SE direction, at a right angle to the flight line direction, with an azimuth of 150° from true north [39]. The tie line spacing was chosen as 16 km intervals. The total magnetic intensity (TMI) was conducted at a nominal sensor altitude of 300 m of terrain clearance [39].

The TMI grid was reduced to the pole (RTP) grid map in order to properly locate the magnetic anomalies across the magnetic source bodies. In the current experiment, residual and regional magnetic component maps were generated from the RTP aeromagnetic data using Fast Fourier transformation (FFT). The RTP aeromagnetic map was further subjected to Tilt Derivative (TDR) and Euler Deconvolution in order to find the characteristics that might be important in mineral prospecting.

The ratio of the potential field's first vertical derivative to its horizontal gradient serves as a proxy for the tilt angle [40]. When employing the zero-contour line to locate the margins of sources at shallow and deep depths, tilt angle derivative (TDR) offers an advantage [40,41]; the tilt derivative (TDR) method is expressed as the following:

$$\text{TDR} = \tan^{-1} \left(\frac{VDR}{HGM} \right) \quad (1)$$

where VDR is the vertical derivative of the magnetic field, and HGM is its horizontal gradient magnitude.

Reid et al. (1990) employed gridded data and generalized the Euler deconvolution to show the position and depth of the magnetic sources. This technique has successfully been utilized for regional interpretation and has proven its effectiveness in identifying lineaments and geological structures (contacts and faults). The authors of [42] suggested modifications to Euler deconvolution for application to magnetic data.

$$\frac{\partial T}{\partial x} (x - x_0) + \frac{\partial T}{\partial y} (y - y_0) + \frac{\partial T}{\partial z} (z - z_0) = N(B - T) \quad (2)$$

where T is the total field detected at (x, y, z) by the magnetic source at position (x_0, y_0, z_0) , B is the background value of the total field, and N is the degree of homogeneity or geophysics related to the structural index (SI).

In the current study, aeromagnetic data were gridded, processed, and mapped using the Geosoft Oasis Montaj program. Furthermore, the results obtained from structural lineaments were presented as rose diagrams using the RockWorks program.

4. Results and Discussion

The total aeromagnetic (TM) map (Figure 2) shows positive and negative magnetic anomalies. The positive anomalies vary from 2.6 nT to 220.9 nT with orange, red, and magenta colors. The highest positive magnetic anomalies (more than 47.7 nT to 220.9 nT) occupy the central, southeast-central, western, eastern, and northern parts. The negative magnetic anomalies (−7.8 nT to −288.3 nT) are characterized by yellow, green, and light-to-deep-blue colors (Figure 2). The western region is home to the highest negative magnetic anomalies, which extend from −288.3 nT to −95.9 nT (Figure 2).

The RTP map (Figure 3) displays the range of magnetic values, which range in size, shape, and magnitude from −312.4 to 209.6 nT. These anomalies generally follow the NNW–SSE (Red Sea axis trend), NE–SW, and NNE–SSW trends. It is possible that hidden faults, shear zones, or subsurface dikes are the cause of the NNW–SSE negative and positive magnetic anomalies (Figure 3). In the center of the research region, the position of Au and Ba mineralization was connected to this trend. According to [43], the NNW–SSE linear magnetic anomalies in the Kingdom of Saudi Arabia are related to mineralization.

Gridded RTP magnetic data were used to determine the 2D power spectrum (Figure 4). An examination of the power spectrum curve reveals the frequency of the near-surface and deep magnetic components. The shallow and deep magnetic sources are thought to have typical depths of 80 m and 570 m, respectively (Figure 4).

When looking at the high-pass (residual) map (Figure 5) of RTP data, it is possible to see a number of different negative and positive magnetic anomalies with varying amplitudes and frequencies, trending in the NNW–SSE, ENE–WSW, and NE–SW directions. These anomalies are dissected by many faults in different directions. In addition, this map confirms the existence of negative linear magnetic anomalies (−36.6 nT to −137.3 nT) at this depth (80 m). The negative and positive magnetic anomalies are depicted on the low-pass (regional) map of RTP data with varying amplitudes and frequencies (Figure 6). They are trending in the NNW–SSE and NE–SW directions.

The TDR filter was applied to the RTP grid to highlight structures such as faults and contacts to help in the mineral exploration research, to find magnetic sources' edges. The

zero-contour line, which shows the location of changes in magnetic susceptibility on the TDR map (Figure 7), is highlighted.

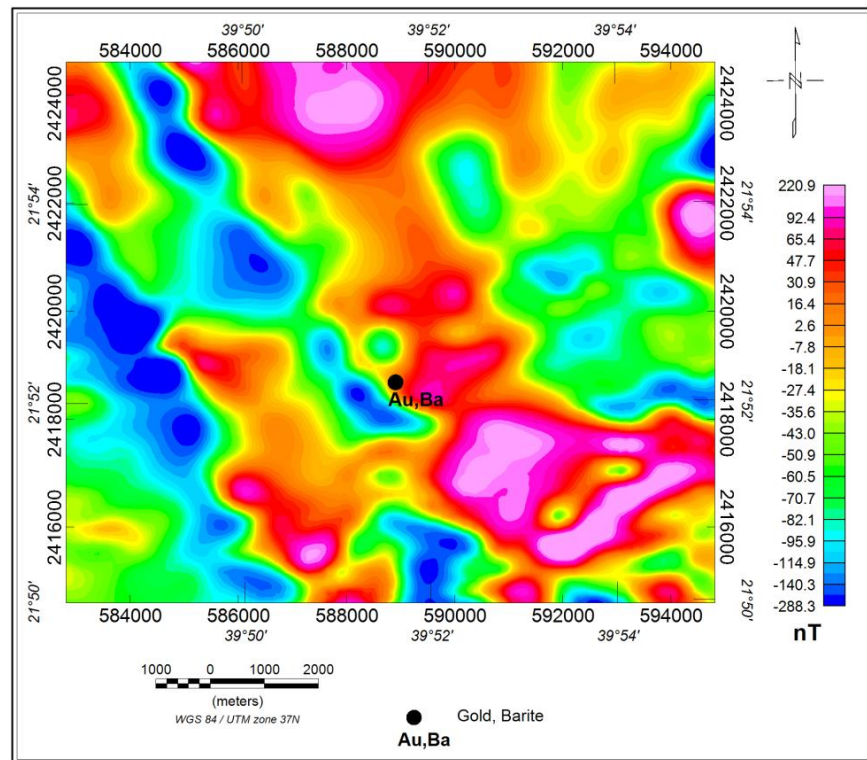


Figure 2. Total intensity aeromagnetic map, Harrat ad Danun area, Kingdom of Saudi Arabia (Aero Service, 1966).

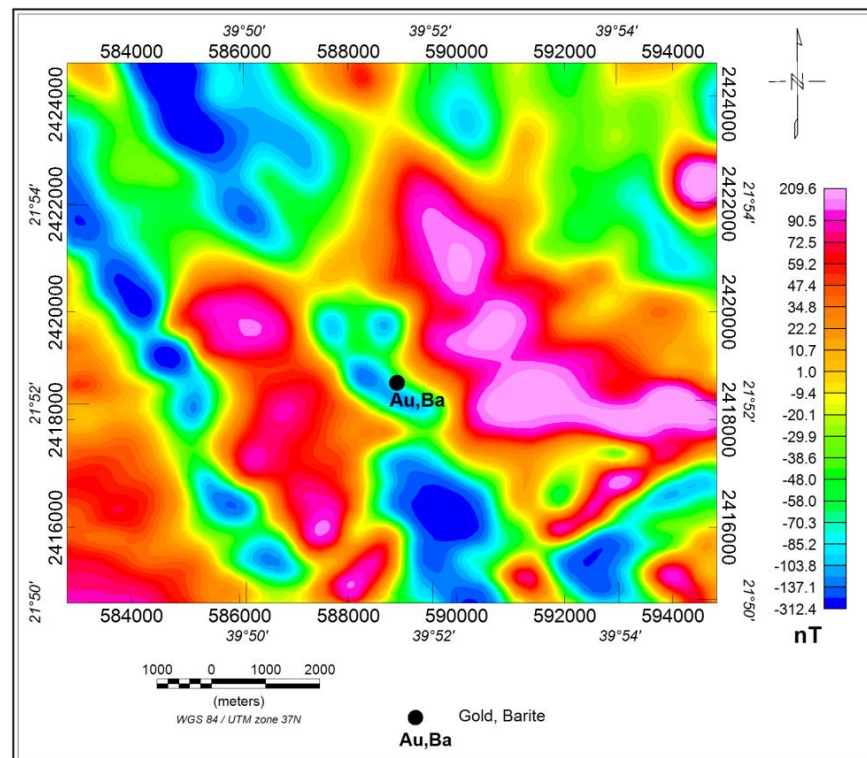


Figure 3. Reduction to the pole (RTP) aeromagnetic map, Harrat ad Danun area, Kingdom of Saudi Arabia (Aero Service, 1966).

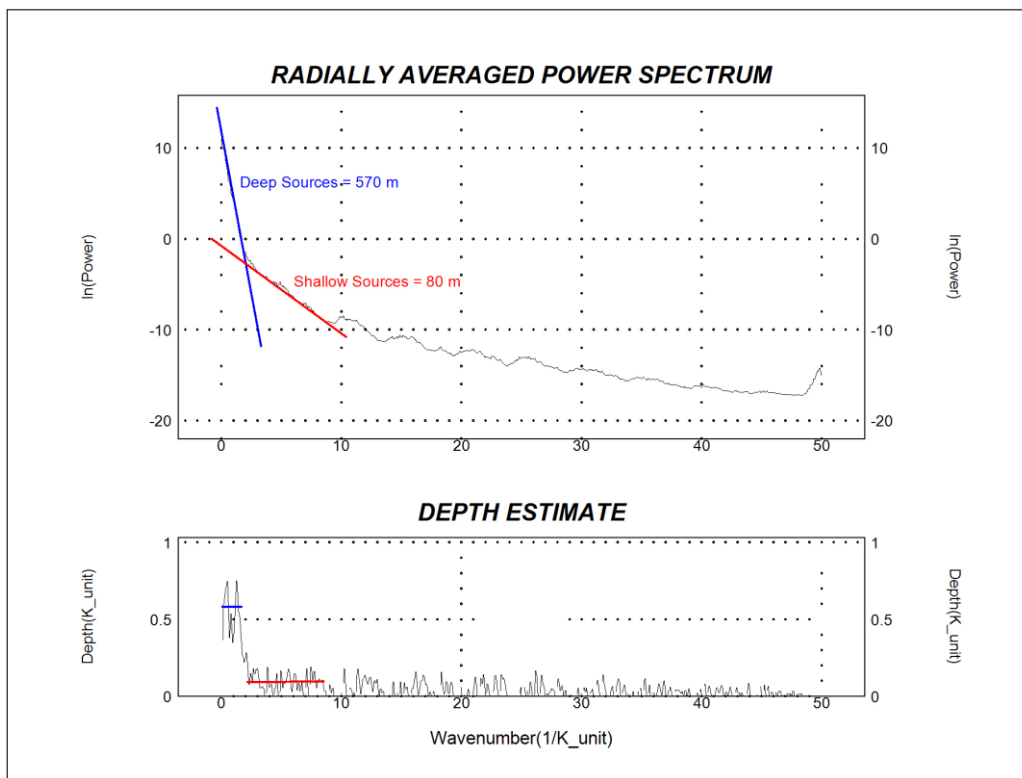


Figure 4. Radially averaged power spectrum and depth estimate from RTP aeromagnetic map, Harrat ad Danun area, Kingdom of Saudi Arabia.

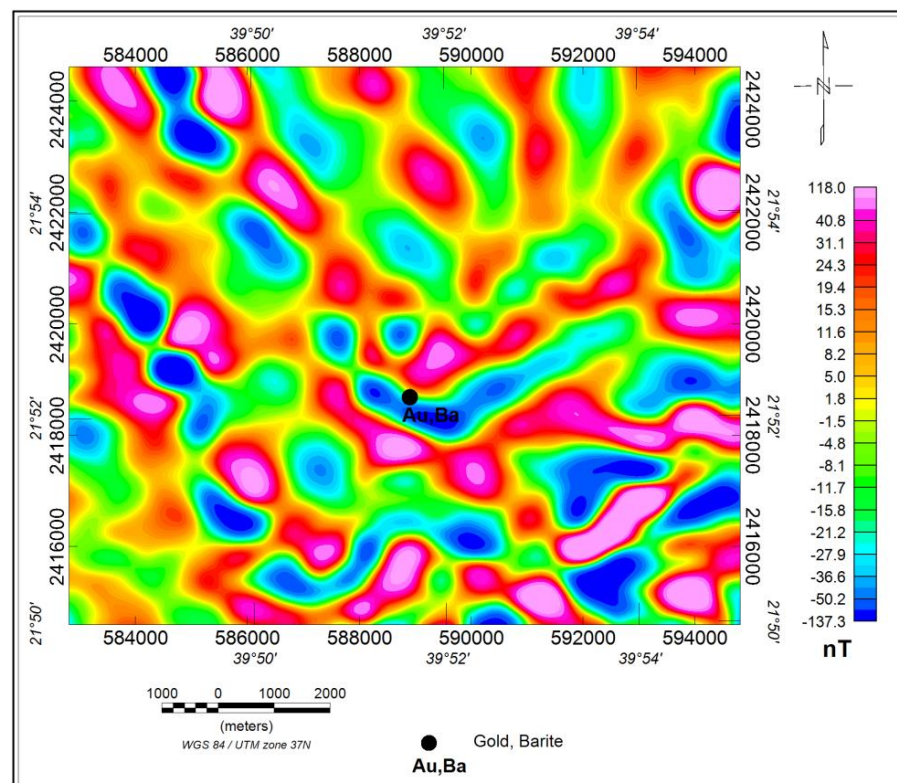


Figure 5. High-pass filtered (residual) aeromagnetic map at 80 m depth, Harrat ad Danun area, Kingdom of Saudi Arabia.

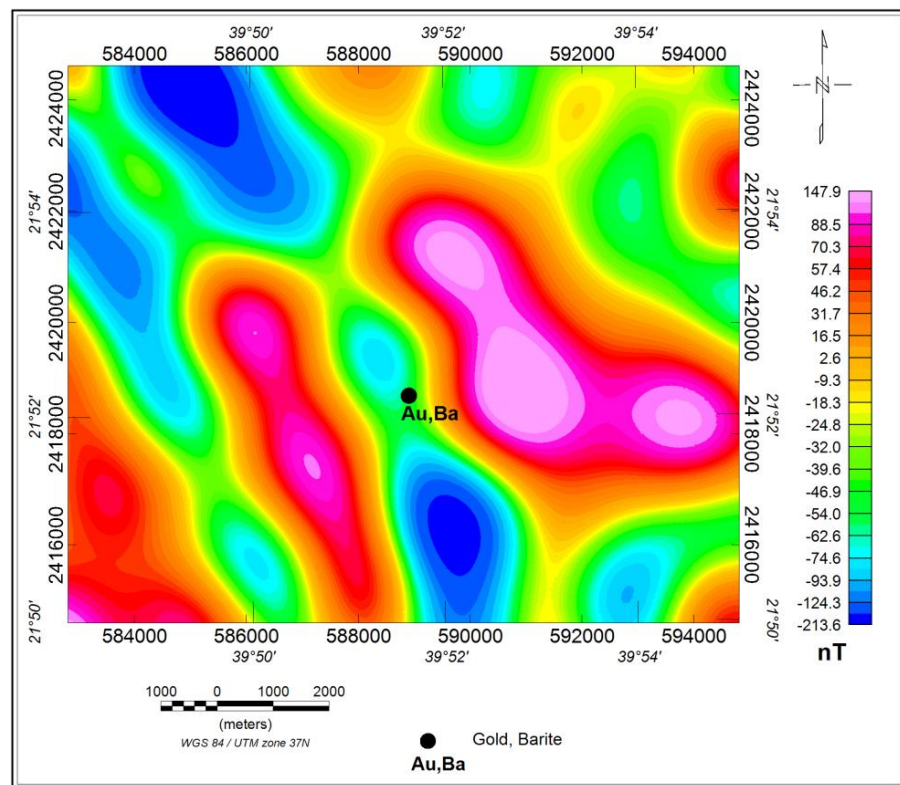


Figure 6. Low-pass filtered (regional) aeromagnetic map at 570 m depth, Harrat ad Danun area, Kingdom of Saudi Arabia.

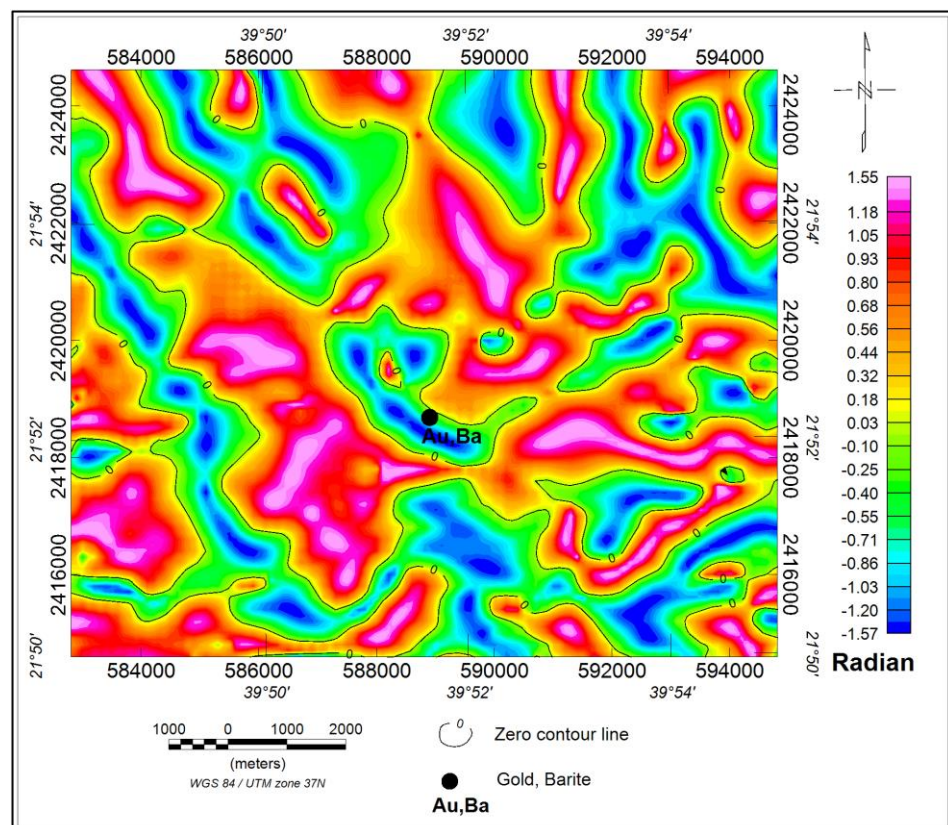


Figure 7. Tilt Derivative (TDR) aeromagnetic map, Harrat ad Danun area, Kingdom of Saudi Arabia.

The research area’s RTP aeromagnetic data grid was subjected to the Euler deconvolution algorithm. The lower structural indices from 0 to 1 are superior depth estimators, as [44] showed. In order to characterize connections and faults in the regional interpretation of the study area, one structural indicator (SI) with a value of 0.0 has been chosen. The Euler deconvolution technique’s produced findings are shown as colored circles placed on maps to show the source position and depth.

The Euler map (Figure 8) was created by applying Euler deconvolution with SI = 0.0, which displays clusters of circles in linear and curved shapes to represent the nature of probable contacts between the rock units. It is believed that faults or contacts with depths between 1 and 474 m are what caused the linear clustering rings.

In the studied area, the linear solutions of depths (1 m–208 m) are widely dispersed (Figure 8). The main trends of these solutions are NNW–SSE, NW–SE, NE–SW, and NNE–SSW. These solutions relate to contacts and faults (Figures 3 and 8). While this examination was being carried out, it was discovered that several areas of the negative and positive magnetic anomalies, particularly in the western, eastern, southern, northern, and central areas (Figures 3 and 8), were associated with solutions that have depths between 208 m and 474 m (Figures 3 and 8).

The subsurface features (faults) that impacted the research area are depicted in Figure 9 by converting the zero-contour lines of the TDR map to lineaments. It is concluded that the primary structures in the study region are represented by the NNW–SSE, NE–SW, and NNE–SSW tendencies (Figure 9). It is notable that it was found that the majority of felsic and mafic dikes are connected to subterranean structures by comparing the geological map (Figure 1) with the TDR map and its lineaments (Figures 7 and 9). According to Figure 10’s analysis of lineament structures using Euler deconvolution, the research area is impacted by three structural trends: WNW–ESE, NNE–SSW, and NNW–SSE [30].

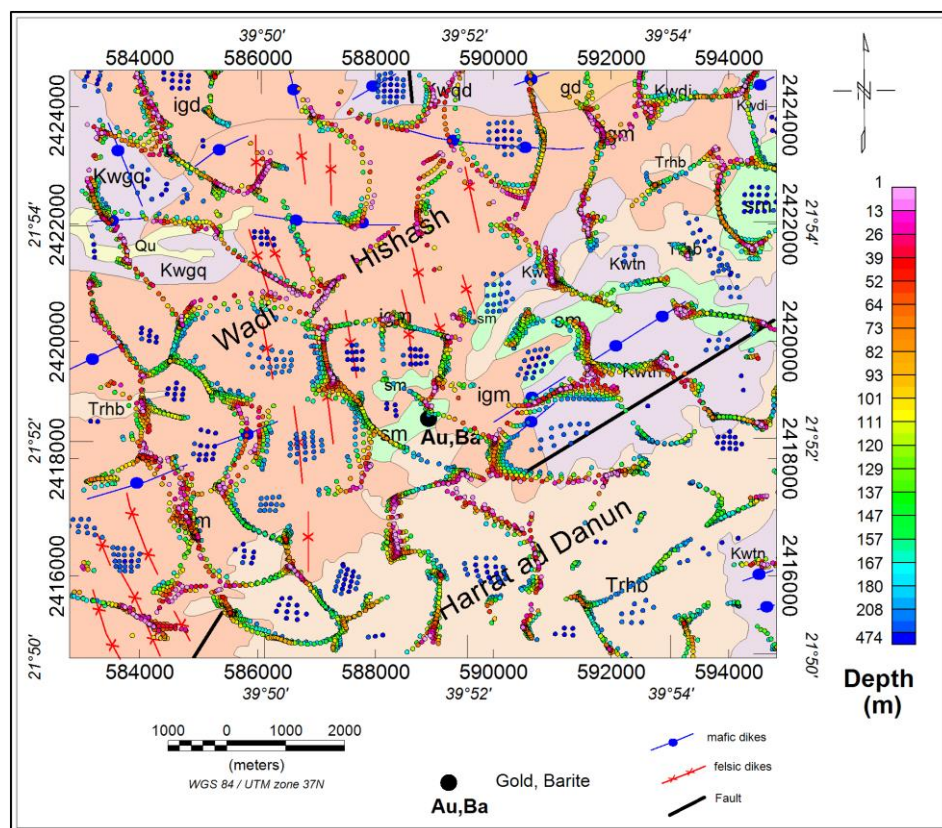


Figure 8. Euler deconvolution solutions with structural index 0.0 (SI = 0.0) of the RTP aeromagnetic map, Harrat ad Danun area, Kingdom of Saudi Arabia. Geologic map as background.

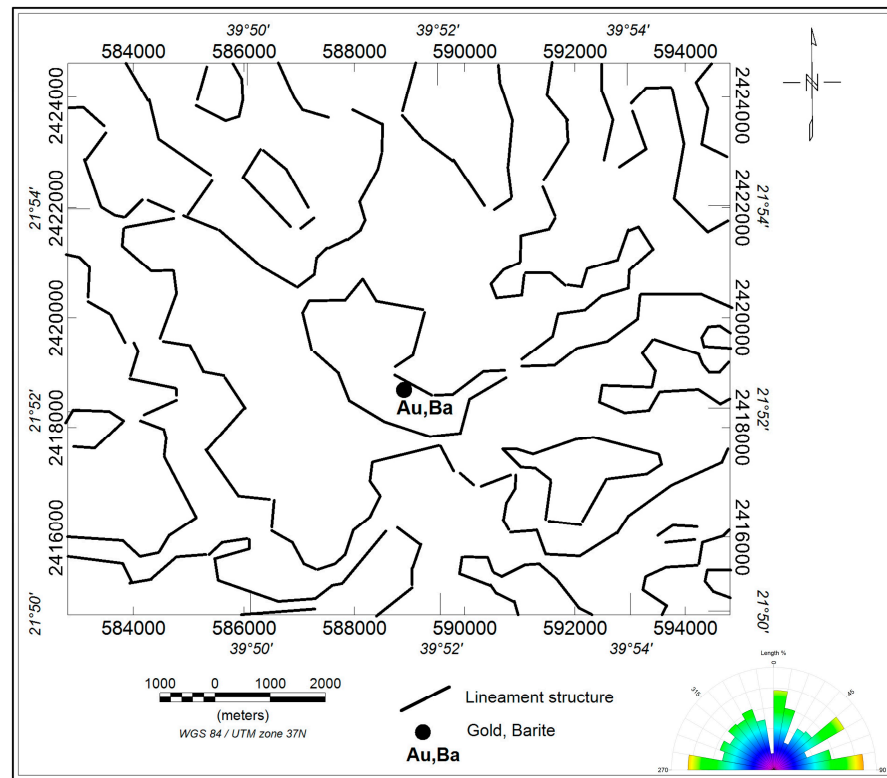


Figure 9. The lineament structures as traced from the TDR aeromagnetic map (Figure 7) and rose diagram (inset), Harrat ad Danun area, Kingdom of Saudi Arabia.

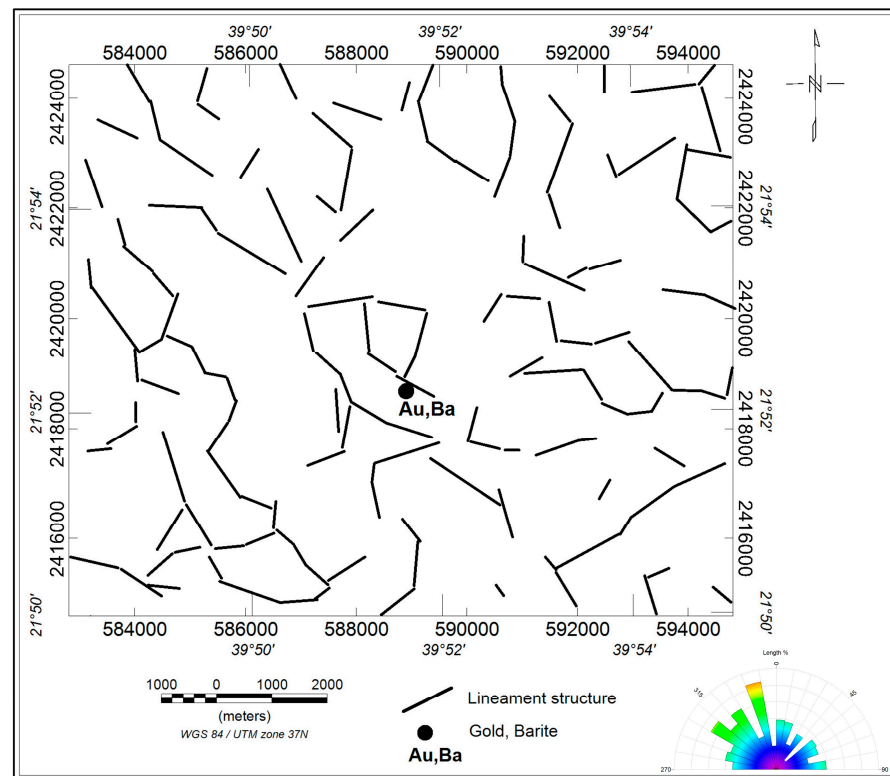


Figure 10. The lineament structures as traced from Euler deconvolution solutions with structural index 0.0 (SI = 0.0) (Figure 8) and rose diagram (inset), Harrat ad Danun area, Kingdom of Saudi Arabia.

Most Au deposits in Saudi Arabia are controlled by major structures and shear zones [29,30,45,46]. The study area's mapped gold and barite mineralization corresponds to a negative magnetic anomaly that is centered there and trends in the Red Sea fault system's NNW–SSE direction, intersecting with the NNE–SSW fault (Figures 3 and 5–7). This may suggest that mineralization is controlled by these two trends. Based on this finding, the NNW negative magnetic feature in the western portion of the area (Figures 3, 5 and 7) may likely contain mineralization. It is clear that mineralization is connected with both source depths of 80 m and 570 m for the residual and regional findings. Moreover, the mineralized zones are connected to the NNW–SSE direction. This is in agreement with the results of [22,43].

5. Conclusions

On the total aeromagnetic (TM) map, alternately distributed positive and negative magnetic anomalies are shown. The reduced to the pole (RTP) map exhibits a range of magnetic values (−312.4 to 209.6 nT) that differ in shape, size, and magnitude. These anomalies' general patterns include NNW–SSE (Red Sea axis trend), NE–SW, and NNE–SSW. Subsurface buried dikes, faults, or shear zones could explain the NNW–SSE linear negative and positive magnetic anomalies. This trend was linked to the presence of Au and Ba mineralization in the research area's center. It is concluded that the principal structures in the studied area are the NNW–SSE, NE–SW, and NNE–SSW tendencies. The gridded RTP magnetic data were used to estimate the 2D power spectrum. The power spectrum curve analysis reveals the frequency of the deep-seated and near-surface magnetic components. The estimated average depths of the shallow and deep magnetic sources are 80 m and 570 m, respectively. A variety of other negative and positive magnetic anomalies with differing amplitudes and frequencies are also visible when comparing the high-pass and low-pass maps, with the majority of them trending in the NNW–SSE, ENE–WSW, and NE–SW directions. Many faults cut through these anomalies in different directions. This map also shows the presence of negative linear magnetic anomalies at this depth (80 m) (−36.6 nT to −137.3 nT). The TDR filter and Euler deconvolution technique were utilized to identify horizontal variations in magnetic susceptibility as well as the source position and depth of magnetic sources. With depths ranging from 1 m to 474 m and orientations in the NNW–SSE, NW–SE, NE–SW, and NNE–SSW directions, the linear clustering rings are thought to be the result of contacts or faults. They exhibit both positive and negative magnetic anomalies, especially in the western, eastern, southern, northern, and central zones.

The majority of felsic and mafic dikes have been discovered to be connected to subsurface structures, demonstrating that three structural trends influence the study area: WNW–ESE, NNE–SSW, and NNW–SSE. This indicates that significant structural and shear zones regulate the majority of the Au deposits in Saudi Arabia. The plotted gold and barite mineralization in the study region corresponds to an area-centered negative magnetic anomaly with an NNW–SSE trend that crosses the NNE–SSW fault. This could imply that these two trends are responsible for mineralization. The NNW negative magnetic feature in the western part of the area is anticipated to have mineralization based on this detection.

A detailed ground magnetic survey should be conducted around possible Au and Ba locations to identify the subsurface structures framework that affected the area. Furthermore, electromagnetic (EM) and induced polarization (IP) surveys should be applied to the existing mineralization (Au, Ba) to explore any subsurface extensions. In addition, geochemical studies should be carried out at the known mineralization (Au, Ba) locations and similar areas to determine the grade of mineralization.

Author Contributions: Conceptualization, A.M.E. and R.A.Y.E.-Q.; methodology, R.A.Y.E.-Q. and K.A.; software, R.A.Y.E.-Q.; validation, A.M.E., P.A. and M.S.F.; formal analysis, K.A.; investigation, A.M.E., R.A.Y.E.-Q. and P.A.; resources, M.S.F.; data curation, R.A.Y.E.-Q.; writing—original draft preparation, R.A.Y.E.-Q., A.M.E., P.A. and K.A.; it writing—review and editing, A.M.E.; visualization,

M.S.F.; supervision, A.M.E.; project administration, A.M.E.; funding acquisition, K.A. and M.S.F. All authors have read and agreed to the published version of the manuscript.

Funding: Deputyship for Research and Innovation, “Ministry of Education” in Saudi Arabia, project no. (IFKSUOR3-192-3).

Data Availability Statement: Not applicable.

Acknowledgments: The authors extend their appreciation to the Deputyship for Research and Innovation, “Ministry of Education” in Saudi Arabia for funding this research through the project no. (IFKSUOR3-192-3).

Conflicts of Interest: The authors declare no conflict of interest.

References

1. DMMR. *Saudi Arabian Directorate General of Mineral Resources. Mineral Resources Activities*; Ministry of Petroleum and Mineral Resources: Riyadh, Saudi Arabia, 1970; pp. 46–70.
2. Darwish, M.A.; Dar Ikram, H.; Abdulaziz, M.I. *Saudi Arabia Starts Up a New Gold Mine at Mahd-Adh-Dahab, E&M/J*; Macgraw-Hill: New York, NY, USA, 1988; pp. 34–38.
3. Darwish, M.A.; Hanif, M. Minerals potential of Saudi Arabia. In Proceedings of the 1st Conference on Indigenous Materials and Their Utilization in the Gulf Region, Kuwait, 1 November 1986.
4. Ibrahim, M. *Big Plans for Mineral Investment in the Kingdom of Saudi Arabia*; The Arab News Daily: Jeddah, Saudi Arabia, 1992.
5. Babhair, A. *Kingdom of Saudi Arabia, A Country Report*; Saudi Geological Survey: Jeddah, Saudi Arabia, 2002.
6. DMMR. *Saudi Arabian Deputy Ministry for Mineral Resources Activities and Achievements 1990–1994*; Ministry of Petroleum and Mineral Resources: Jeddah, Saudi Arabia, 1995.
7. DMMR. *Ministry of Petroleum and Mineral Resources, Saudi Arabian Mineral Resources Annual Report*; Ministry of Petroleum and Mineral Resources: Jeddah, Saudi Arabia, 1984; pp. 13–14.
8. Mudd, G. *The Sustainability of Mining in Australia: Key Production Trends and Their Environmental Implications for the Future*; Research Report No RR5; Department of Civil Engineering, Monash University and Mineral Policy Institute: Melbourne, Australia, 2007.
9. Mudd, G.; Ward, J. Will Sustainability Constraints Cause ‘Peak Minerals’? In Proceedings of the 3rd International Conference on Sustainability Engineering and Science: Blueprints for Sustainable Infrastructure, Auckland, New Zealand, 9–12 December 2008.
10. Darwish, M.A.; Butt, N.A. Mineral Resource Potential and Its Development in Saudi Arabia. *JKAU Eng. Sci.* **1996**, *8*, 107–120. [[CrossRef](#)]
11. *Fourth Development Plan (1985–1990)*; Ministry of Planning KSA: Riyadh, Saudi Arabia, 1985; pp. 167–184.
12. Davis, G.; Tilton, J. Should Developing Countries Renounce Mining? A Perspective on the Debate, Colorado School of Mines. 2002. Available online: <https://www.icmm.com/uploads/62TiltonDavisfinalversion.pdf> (accessed on 1 April 2023).
13. Togolo, M. Mining and sustainability—Placer Niugini Limited. In Proceedings of the PACRIM’99, International Conference on Earth Science, Exploration and Mining around the Pacific Rim, Bali, Indonesia, 10–13 October 1999.
14. Aldagheiri, M. The minerals sector and sustainable development in Saudi Arabia. In Proceedings of the Sustainable Development Indicators in the Minerals Industry (SDIMI) 2009 Conference, Gold Coast, Australia, 6–8 July 2009. 28p.
15. Alharbi, O.; Amjad, M.; Alabdulaaly, A.; Khater, G.; Alsari, A. Industrial utilization of white silica sandstone in Riyadh area, Saudi Arabia. *Arab. Gulf J. Scient. Res.* **1997**, *15*, 29–39.
16. Al Jahdli, N.S. Geology of Jabal Ghadarah Area, Bi’r Tawilah District with Special Emphasis on Listvinite as a Potential Source for Gold in the Kingdom of Saudi Arabia. Master’s Thesis, King Abdulaziz University, Jeddah, Saudi Arabia, 2004.
17. Harbi, H.A.; EldougDoug, A.A.; Al Jahdali, N.S. Evolution of the Arabian Shield and associated mineralization. In Proceedings of the 9th Arab Conference of Mineral Resources, Jeddah, Saudi Arabia, 30 October–1 November 2006; pp. 1–11.
18. Gabr, S.; Ghulam, A.; Kusky, T. Detecting areas of high-potential gold mineralization using ASTER data. *Ore Geol. Rev.* **2010**, *38*, 59–69. [[CrossRef](#)]
19. Al-Garni, M.A.; Hassanein, H.I.E. Aeromagnetic data analysis to enhance the demonstration of the subsurface mineralized zone occurrences, As-Safra prospect area, Saudi Arabia. *Arab. J. Geosci.* **2010**, *5*, 313–326. [[CrossRef](#)]
20. Surour, A.A.; Harbi, H.M.; Ahmed, A.H. The Bi’r Tawilah deposit, central western Saudi Arabia: Supergene enrichment of a Pan-African epithermal gold mineralization. *J. Afr. Earth Sci.* **2014**, *89*, 149–163. [[CrossRef](#)]
21. Torres, J.E.A. The Potential for CO₂ Disposal in Western Saudi Arabia: The Jizan Group Basalts. Master’s Thesis, King Abdullah University of Science and Technology, Thuwal, Saudi Arabia, 2020.
22. Eldsouky, A.M.; El-Qassas, R.A.Y.; Pham, L.T.; Abdelrahman, K.; Alhumimidi, M.S.; El Bahrawy, A.; Mickus, K.; Sehsah, H. Mapping Main Structures and Related Mineralization of the Arabian Shield (Saudi Arabia) Using Sharp Edge Detector of Transformed Gravity Data. *Minerals* **2022**, *12*, 71. [[CrossRef](#)]
23. Alsaud, M.M. Structural mapping from high resolution aeromagnetic data in west central Arabian Shield, Saudi Arabia using normalized derivatives. *Arab. J. Geosci.* **2008**, *1*, 129–136. [[CrossRef](#)]
24. Elawadi, E.; Mogren, S.; Ibrahim, E.; Batayneh, A.; Al-Bassam, A. Utilizing potential field data to support delineation of groundwater aquifers in the southern Red Sea coast, Saudi Arabia. *J. Geophys. Eng.* **2012**, *9*, 327–335. [[CrossRef](#)]

25. Alandoonisi, N.; Harbi, H.M.; Atef, A.; Aboualnaga, H.; Rashed, M. Geophysical Assessment of the Environmental Pollution at Downstream of Wadi Uranah, Southwest of Makkah, Saudi Arabia. *Nat. Environ. Pollut. Technol.* **2018**, *17*, 391–398.
26. Abuelnaga, H.S.; Aboulela, H.A.; El-Sawy, E.-S.K.; El Qassas, R.A. Detection of structural setting that controlling Hammam Faroun area, using aeromagnetic and seismicity data, Gulf of Suez, Egypt. *J. Afr. Earth Sci.* **2019**, *158*, 103560. [[CrossRef](#)]
27. Assran, A.; El Qassas, R.; Yousef, M. Detection of prospective areas for mineralization deposits using image analysis technique of aeromagnetic data around Marsa Alam-Idfu road, Eastern Desert, Egypt. *Egypt. J. Pet.* **2019**, *28*, 61–69. [[CrossRef](#)]
28. Eldosouky, A.M.; Pham, L.T.; Hassan, P.; Pradhan, M.B. A comparative study of THG, AS, TA, Theta, TDX, and LTHG techniques for improving source boundaries detection of magnetic data using synthetic models: A case study from G. Um Monqul, North Eastern Desert, Egypt. *J. Afr. Earth Sci.* **2020**, *170*, 103940. [[CrossRef](#)]
29. Eldosouky, A.M.; El-Qassas, R.A.; Pour, A.B.; Mohamed, H.; Sekandari, M. Integration of ASTER satellite imagery and 3D inversion of aeromagnetic data for deep mineral exploration. *Adv. Space Res.* **2021**, *68*, 3641–3662. [[CrossRef](#)]
30. Eldosouky, A.M.; Pham, L.T.; El-Qassas, R.A.Y.; Hamimi, Z.; Oksum, E. Lithospheric Structure of the Arabian-Nubian Shield Using Satellite Potential Field Data. In *The Geology of the Arabian-Nubian Shield; Regional Geology Reviews*; Hamimi, Z., Fowler, A.R., Liégeois, J.P., Collins, A., Abdelsalam, M.G., Abd El-Wahed, M., Eds.; Springer: Cham, Switzerland, 2021.
31. El-Qassas, R.A.Y.; Ahmed, S.B.; Abd-ElSalam, H.F.; Abu-Donia, A.M. Integrating of Remote Sensing and Airborne Magnetic Data to Outline the Geologic Structural Lineaments That Controlled Mineralization Deposits for the Area around Gabal El-Niteishat, Central Eastern Desert, Egypt. *Geomaterials* **2021**, *11*, 1–21. [[CrossRef](#)]
32. El-Qassas, R.A.Y.; Abu-Donia, A.M.; Omar, A.E.A. Delineation of hydrothermal alteration zones associated with mineral deposits, using remote sensing and airborne geophysics data. A case study: El-Bakriya area, Central Eastern Desert, Egypt. *Acta Geod. Geophys.* **2023**, *58*, 71–107. [[CrossRef](#)]
33. Elkhateeb, S.O.; Eldosouky, A.M.; Khalifa, M.O.; Aboalhassan, M. Probability of mineral occurrence in the Southeast of Aswan area, Egypt, from the analysis of aeromagnetic data. *Arab. J. Geosci.* **2021**, *14*, 1514. [[CrossRef](#)]
34. Kharbish, S.; Eldosouky, A.M.; Amer, O. Integrating mineralogy, geochemistry and aeromagnetic data for detecting Fe–Ti ore deposits bearing layered mafic intrusion, Akab El-Negum, Eastern Desert, Egypt. *Sci. Rep.* **2022**, *12*, 15474. [[CrossRef](#)]
35. Ekwok, S.E.; Akpan, A.E.; Achadu, O.-I.M.; Thompson, C.E.; Eldosouky, A.M.; Abdelrahman, K.; Andráš, P. Towards Understanding the Source of Brine Mineralization in Southeast Nigeria: Evidence from High-Resolution Airborne Magnetic and Gravity Data. *Minerals* **2022**, *12*, 146. [[CrossRef](#)]
36. Mahdi, A.M.; Eldosouky, A.M.; El Khateeb, S.O.; Youssef, A.M.; Saad, A.A. Integration of remote sensing and geophysical data for the extraction of hydrothermal alteration zones and lineaments; Gabal Shilman basement area, Southeastern Desert, Egypt. *J. Afr. Earth Sci.* **2022**, *194*, 104640. [[CrossRef](#)]
37. Moore, T.A.; Al-Rehaili, M.H. Explanatory Notes to the Geologic Map of the Makkah Quadrangle, Sheet21d, Kingdom of Saudi Arabia: Saudi Arabian Dir. Gen. Min. Res. Geoscience Map GM-107C, 1:250,000 Scale. 1989. Available online: <https://www.sciarp.org/%28S%28ceh2tfqyw2orz553k1w0r45%29%29/reference/referencespapers.aspx?referenceid=2170065> (accessed on 1 April 2023).
38. El-Hames, A.S. Determination of groundwater availability in shallow arid region aquifers utilizing GIS technology: A case study in Hada Al-Sham, Western Saudi Arabia. *Hydrogeol. J.* **2004**, *13*, 640–648. [[CrossRef](#)]
39. Aero Service. *Final Operational Report of Airborne Magnetic*; Arabian Geophysical and Surveying Company: Dhahran, Saudi Arabia, 1966.
40. Miller, H.G.; Singh, V. Potential field tilt—A new concept for location of potential field sources. *J. Appl. Geophys.* **1994**, *32*, 213–217. [[CrossRef](#)]
41. Salem, A.; Williams, S.; Fairhead, D.; Smith, R.; Ravat, D. Interpretation of magnetic data using tilt-angle derivatives. *Geophysics* **2008**, *73*, L1–L10. [[CrossRef](#)]
42. Barbosa, V.; Silva, J.B.C.; Medeiros, W.E. Stability analysis and improvement of structural index estimation in Euler deconvolution. *Geophysics* **1999**, *64*, 48–60. [[CrossRef](#)]
43. Dadet, P.; Marchesseau, J.; Millon, R.; Motti, E. Mineral occurrences related to stratigraphy and tectonics in Tertiary sediments near Umm Lajj, eastern Red Sea area, Saudi Arabia. *Philos. Trans. R. Soc. Lond. Ser. A* **1970**, *267*, 99–106.
44. Reid, A.B.; Allsop, J.M.; Granser, H.; Millett, A.J.; Somerton, I.W. Magnetic interpretation in three dimensions using Euler deconvolution. *Geophysics* **1990**, *55*, 80–91. [[CrossRef](#)]
45. Bonnemaïson, M.; Marcoux, E. Auriferous mineralization in some shear-zones: A three-stage model of metallogenesis. *Miner. Deposita* **1990**, *25*, 96–104. [[CrossRef](#)]
46. Eldosouky, A.M.; Elkhateeb, S.O.; Mahdy, A.M.; Saad, A.A.; Fnais, M.S.; Abdelrahman, K.; Andráš, P. Structural analysis and basement topography of Gabal Shilman area, South Eastern Desert of Egypt, using aeromagnetic data. *J. King Saud Univ. Sci.* **2021**, *34*, 101764. [[CrossRef](#)]

Disclaimer/Publisher’s Note: The statements, opinions and data contained in all publications are solely those of the individual author(s) and contributor(s) and not of MDPI and/or the editor(s). MDPI and/or the editor(s) disclaim responsibility for any injury to people or property resulting from any ideas, methods, instructions or products referred to in the content.